Contents lists available at SciOpen

Food Science and Human Wellness

journal homepage: https://www.sciopen.com/journal/2097-0765

China Food Publishing Co.

Preparation and characterization of microalgae-derived extracellular vesicles and their protective effect on acute alcohol-induced liver injury

Jiawen Song[a], Lei Zhou[a], Shengfeng Peng[b,*], David Julian McClements[c], Wei Liu[a,*]

[a]State Key Laboratory of Food Science and Resources, Nanchang University, Nanchang 330047, China
[b]Department of Rehabilitation Medicine, the Second Affiliated Hospital of Nanchang University, Nanchang University, Nanchang 330006, China
[c]Biopolymers and Colloids Laboratory, Department of Food Science, University of Massachusetts, Amherst 01003, USA

ARTICLE INFO

Article history:
Received 11 September 2024
Received in revised form 27 October 2024
Accepted 18 November 2024

Keywords:
Alcohol-induced liver injury
Microalgae
Extracellular vesicles
Nrf2/HO-1 signaling pathway
Gut microbiota

ABSTRACT

Increased levels of alcohol consumption are linked to an increased risk of alcoholic liver disease. As a novel source of national food, microalgae are rich in bioactives and have been demonstrated to confer benefits to human health. The effects of microalgae extracellular vesicles (M-EVs) on alcohol-induced liver injury have not been studied previously. In this study, 3 types of M-EVs were isolated using a combination of tangential flow filtration (TFF) and size exclusion chromatography (SEC). The structure and composition of M-EVs were characterized and the safety and liver-accumulation of M-EVs were also confirmed. Results shown that 3 types M-EVs were shown to be colloidal particles ((198.9 ± 7.2), (191.7 ± 5.1), and (259.5 ± 8.1) nm) with negative charge ((–25.0 ± 1.6), (–21.4 ± 0.6), and (–22.4 ± 1.6) mV). M-EVs were able to reduce the levels of alanine aminotransferase (ALT), aspartate aminotransferase (AST), alkaline phosphatase (ALP), and triglycerides (TGs) in the mice and regulated the levels of malondialdehyde (MDA), glutathione (GSH), and superoxide dismutase (SOD), which protected the mice against oxidative damage and inflammation caused by alcohol-induced liver injury. In addition, the M-EVs may also have alleviated alcohol-induced liver injury through activation of the Nrf2/HO-1 signaling pathway and regulation of CYP2E1 expression, as well as by modulating the diversity and composition of the gut microbiota. The potentially beneficial effects of M-EVs on alcoholic liver disease may provide a theoretical basis for further exploration of the health function of M-EVs in the food industry.

1. Introduction

Increased consumption of alcohol has been linked to an increased risk of liver disease, including alcoholic liver disease (ALD)[1]. As the primary organ for alcohol metabolism, the liver develops cirrhosis, fibrosis, steatosis, and alcoholic-associated hepatitis as a result of acute or excessive alcohol abuse. Oxidative stress and inflammatory injury have been implicated in the pathogenesis of ALD in numerous studies[2-4]. Clinically, anti-inflammation drugs (such as glucocorticoids) are widely used to treat ALD, but their long-term use can lead to adverse side effects[5]. There is therefore great interest in developing more natural alternatives for the prevention and treatment of ALD. As an innovative food source, microalgae contain nutrients and other bioactive compounds such as proteins, lipids carbohydrates, vitamins, pigments, and flavors[6-8]. Microalgae are already used in the medical care[9], food industry[10], cosmetics[11], and agricultural fields[12] as a source of nutrients and bioactives. Some studies have shown that *Chlorella*, *Spirulina platensis*, and *Haematococcus* exhibit potentially beneficial bioactive properties including antioxidant, anti-inflammatory, and anticancer activities[13-15]. Indeed, some bioactive compounds extracted from microalgae have been shown to be effective at treating certain diseases[16-17]. For example, astaxanthin exhibits antioxidant and anti-inflammatory properties by modulating nuclear factor κB (NF-κB) in the treatment of ALD[18]. Researchers have therefore been exploring the potential of various microalgae-derived bioactive compounds for the treatment of different diseases[7].

* Corresponding author at: College of Food Science, Shihezi University, Shihezi 832000, China.
E-mail address: pengsf@ncu.edu.cn (S.F. Peng); liuwei@ncu.edu.cn (W. Liu)
Peer review under responsibility of Beijing Academy of Food Sciences.

SciOpen Publishing services by Tsinghua University Press

http://doi.org/10.26599/FSHW.2025.9250468

Extracellular vesicles (EVs) are natural active components that can be isolated from microalgae and serve as important transporters for biomolecules[19-20]. EVs are spheroidal colloidal particles (50–1 000 nm) with a phospholipid bilayer membrane, which are enriched with a range of nucleic acids, proteins, lipids, and metabolic molecules[21]. Several advantageous biological properties, such as immunomodulatory, antioxidant, and anti-inflammatory properties, have been found in EVs[22-26]. For example, EVs in ginger attenuate acute liver injury by inhibiting the generation of reactive oxygen species (ROS) and activating the activation of genes related to liver detoxification and antioxidant defense[27]. For oral delivery applications, EVs are typically extracted from edible plants, such as ginseng[28], grapes[29], and tomatoes[30], but they can also be extracted from microalgae[31]. Substantial quantities of EVs-rich algal fluids are typically discarded as waste during the manufacture of microalgae products, which has prompted research into its potential of microalgae as a source for stable mass production of EVs[32]. Moreover, a variety of isolation techniques have been employed to obtain to isolate microalgae extracellular vesicles (M-EVs) from waste materials[33-35]. Nevertheless, the potential of M-EVs as a therapeutic agent for ALD remains unexplored.

In our study, extracellular vesicles from 3 commonly cultured microalgae, *Scenedesmus* sp. (Sc-EVs), *Chlorella* sp. (Ch-EVs), and *Spirulina* sp. (Sp-EVs), were isolated and purified using a combination of tangential flow filtration (TFF) and size exclusion chromatography (SEC). The composition, structure, and properties of these M-EVs were then characterized. Finally, the potential mechanisms of action of M-EVs were assessed, including their ability to reduce liver oxidative stress and inflammation using an ALD mice model. The results of this study could lead to the development of novel nature-derived functional foods, supplements, or pharmaceutical formulations to treat alcohol-related diseases.

2. Materials and methods

2.1 Materials

Nanjing Jiancheng Bioengineering Institute (Nanjing, China) provided the assay kits for measuring the following enzymes: glutathione peroxidase (GSH-Px), alanine aminotransferase (ALT), aspartate aminotransferase (AST), alkaline phosphatase (ALP), bicinchoninic acid (BCA), malondialdehyde (MDA), triglycerides (TGs), and superoxide dismutase (SOD). We bought kits for the enzyme-linked immunosorbent test (ELISA) from Jiangsu Meimian Industrial Co., Ltd. (Jiangsu, China).

2.2 Cultivation of microalgae

Microalgae were grown in flasks containing 2 000 mL of nutrient medium. *Scenedesmus* sp. and *Chlorella* sp. were grown in blue-green medium. *Spirulina* sp. was grown in zarrouk medium. These microalgae were cultured into exponential growth phase (approximately 5×10^5 cell/mL) and then expanded at a ratio of 1:9 (*V*/*V*). Microalgae were cultivated at a temperature of 22–24 ℃, a light intensity of 100–300 $\mu E/m^2 \cdot s^{-1}$ for 24 h. The microalgae were collected for further use after a 15-day cycle. The culture mediums were obtained from Guangyu Biological Technology Co., Ltd. (Shanghai, China).

2.3 Isolation and purification by a TFF-SEC combination method

Initially, algal scum and impurities were removed by centrifugation at 10 000 × *g* for 30 min at 4 °C. TFF with a 10-kDa molecular weight cut-off (MWCO) ultrafiltration membrane filter was then used to concentrate the supernatants. SEC, filled with Sepharose CL-4B, was then used to gather and purify the concentrations of Sc-EVs, Ch-EVs, and Sp-EVs. The protein concentration of the concentrated and purified samples obtained using this procedure were determined using a BCA assay kit.

2.4 Particle size, Zeta potential, and concentration analysis

The Malvern Zetasizer Nano-ZSP (Zetasizer™ Nano-ZSP, Malvern Panalytical Ltd., Malvern, Worcestershire, UK) was employed for the measurement of the samples' average particle diameter and Zeta potential[36]. A nanoparticle tracking analysis (NTA) device (NanoSight™ NS300, Malvern Panalytical Ltd., Malvern, Worcestershire, UK) was used to evaluate the samples' concentration and particle size distribution. All samples were repeated in triplicates and analyzed by the instrument software (NTA 2.3).

2.5 Transmission electron microscopy (TEM) analysis

The samples were put on a copper grid coated with carbon (200 mesh), and 2% uranyl acetate was used to negatively stain them in order to analyze their morphology. Following a 30 s staining period, the mesh was rinsed with distilled water. After drying, the sample was examined with a TEM device (JEM-1200EX, JEOL Ltd., Akishima, Tokyo, Japan).

2.6 Lipids and protein analysis

Lipids were extracted from the M-EVs by mixing them with a methanol/chloroform (2:1, *V*/*V*) solution. Liquid chromatography-mass spectrometry (LC-MS) (Orbitrap Exploris™ 120, Thermo Fisher Scientific Inc., Waltham, USA) was then used to quantify the amount of lipids. The lipid content was then ascertained by analyzing the data using Proteo Wizard software (version 3.0.9, msConvert tool).

Information about the protein composition of the M-EVs was obtained using sodium dodecyl sulfate polyacrylamide gel electrophoresis (SDS-PAGE). Samples proteins were separated electrophoretically on a pre-prepared Novex Bolt 4%–12% Bis-Tris Plus gel under reducing conditions. Colloidal Coomassie Blue was used to stain the samples after separation to identify the location of the proteins.

2.7 In vitro cell viability of M-EVs

An *in vitro* cell viability experiment was used to evaluate the M-EVs potential toxicity. M-EVs (1×10^6 and 1×10^7 particles/mL) were co-incubated with Caco-2 cells in the 96-well plate for 24 h. The CCK8 assay was performed and the values of the different concentrations of samples were measured using an enzyme-labeling apparatus at 450 nm.

2.8 Biodistribution of M-EVs in mice

The biodistribution of M-EVs in mice was determined by oral administration of DIR-labeled Ch-EVs, Sp-EVs, and Sc-EVs into healthy female C57BL/6 mice (10–12 weeks old). The mice were euthanized 24 h after oral administration of the EVs, and then the organs were collected and analyzed. Using an *in vivo* imaging system (IVIS® Lumina III, PerkinElmer, Inc., Waltham, MA, USA) and *in vivo* imaging analysis software (Living Image® software, version 4.7.2, PerkinElmer, Inc., USA), the intensity of the DIR signal from the various organs was assessed.

2.9 Animal experiments

2.9.1 Establishment of acute alcoholic liver injury model

The C57BL/6 female mice (10–12 weeks) were acquired from SPF Biotechnology Co., Ltd. (Beijing, China). All animals were then housed under a comfortable environment and given ample food and water. The Nanchang University Institutional Animal Care and Use Committee gave its approval to the animal procedures (SYXK (Gan) 2021–0004). All principles in this study adhered to the rules governing the ethical use of animals.

After 1 week of regular feeding, 5 groups (n = 6) of C57BL/6 female mice were randomly assigned. PBS was gavaged daily to the animals in the ethanol group (EtOH) and the control group (CON). Animals in the 3 M-EVs treated groups were orally administered Sc-EVs, Ch-EVs or Sp-EVs for 10 days. All treatment agents including PBS (200 μL) were administered to mice by intragastric administration twice a day. The mice's body weights were noted each day. The CON group received Lieber-DeCarli diets every day. The EtOH, Sc-EVs, Ch-EVs, and Sp-EVs groups received a liquid diet with 0%–4% (*V*/*V*) ethanol from day 1 to 5 (the first 5 days were the alcohol adaptation period), and a liquid diet with 4.7% (*V*/*V*) ethanol from day 5 to day 10. On day 11, the CON group was gavaged with 45% (*m*/*V*) dextrin solutions (9 g/kg body weight), whereas the other groups were gavaged with 31.5% (*m*/*V*) ethanol solutions (5 g/kg body weight). Each mouse was euthanized after 9 h, the sample was centrifuged for 15 min at 3 500 r/min in order to extract the serum. The organs were harvested and weighed. All collected samples were stored at –80 °C. The organ index was calculated for each animal as follows:

$$\text{Organ index (\%)} = \frac{\text{Organ weight (g)}}{\text{Body weight (g)}} \times 100 \quad (1)$$

2.9.2 Serum and liver biochemical parameters assays

BCA assay was used to determine the total protein level. The ALT, AST, ALP, TG, GSH, MDA, and SOD levels were measured using commercial assay kits. Quantification of the levels of TNF-α, IL-1β, IL-6, and IL-10 was conducted using ELISA kits procured from Jiangsu Meimian Industrial Co., Ltd. (Yancheng, China).

2.9.3 Hematoxylin-eosin (H&E) staining

After being preserved for 24 h in a 4% paraformaldehyde solution, fresh mouse liver was embedded in paraffin. After being cut into thick pieces (10 μm), liver slices were stained with H&E. Finally, the images were taken using a 200× magnification digital microscope (DSX1000, Olympus Co., Hachioji, Tokyo, Japan).

2.9.4 Immunofluorescence assays

Paraffin-embedded tissues were deparaffinized. Each thin section was then incubated with goat serum for 30 min at 25 °C. They were then covered with rabbit antibody solution, diluted in PBS, and incubated for 1 h at 25 °C. Following a PBS wash, sections were incubated for 2 h at 25 °C with an Alexa Fluor 488-coupled anti-rabbit secondary antibody. The Sections were cleaned with PBS, dried, and then treated with 4′,6-diamidino-2-phenylindole (DAPI) (Cat. No. G1012, Servicebio, Wuhan, China). An Olympus fluorescent microscope was used to view the sections, and a digital camera (ORCA-Fusion BT, C15440-20UP, Hamamatsu Photonics K.K., Hamamatsu, Japan) was used to take pictures.

2.9.5 Gut microbiota analysis

Approximately 0.1 g of feces was obtained from the colon and analyzed using 16S rRNA gene sequencing reads. The procedures for DNA extraction and RNA gene sequencing were conducted in accordance with the methodology previously described[37]. Operational taxonomic units (OTUs) were identified by Majorbio Biopharm Technology Co., Ltd. (Shanghai, China). The classification of representative sequences for each OTU was also analyzed against the 16S rRNA database. All data were calculated using the built-in commands.

2.9.6 Western blot analysis

The livers were homogenized and centrifuged at 14 000 r/min at 4 °C for 15 min. The protein solutions were then subjected to SDS-PAGE separation and then transferred to the membranes. After blocking, the membranes were probed with antibodies at 4 °C. Specific primary antibodies were then determined, including CYP2E2, nuclear factor erythroid 2-related factor 2 (Nrf2), heme oxygenase-1 (HO-1), and β-actin. After 2 h of incubation, the secondary antibody film was subjected to Western blotting using ECL chemiluminescence kits. Imaging was carried out using Immunostar Zeta (Wako Pure Chemical Industries Ltd., Osaka, Japan). The strips' density was examined using image analysis software (ImageJ, version 1.53t, National Institutes of Health, USA).

2.10 Statistical analysis

All measurements and experiments were performed at least 3 times, and the mean ± standard deviation (SD) is used to report the results. GraphPad Prism (GraphPad Prism 10) and SPSS software (SPSS Statistics 25) were used to examine all statistical data. The least significant difference (LSD) test was used to compare significant differences between samples. $P < 0.05$ was used to determine that the results were statistically significant.

3. Results

3.1 M-EVs isolation and purification by TFF and SEC combined

TFF has been shown to have several advantages for the commercial isolation of substances[19,38]. For this reason, it is often preferred over methods such as ultracentrifugation and normal flow filtration. Ultracentrifugation is time-consuming and costly, and normal flow filtration causes cell rupture and biomolecular precipitation, resulting in low yields and purities[39]. For these reasons, TFF was used to isolate the M-EVs in this study.

The Sc-EVs, Ch-EVs, and Sp-EVs isolated using TFF had average particle diameters of (315 ± 12), (234 ± 13), and (345.6 ± 3.8) nm, respectively, and the average Zeta-potential values were (–17.5 ± 1.5), (–19.9 ± 1.9), and (–12.8 ± 0.6) mV, respectively. After purification using SEC, the average particle diameters of the Sc-EVs, Ch-EVs, and Sp-EVs were (198.9 ± 7.2), (191.7 ± 5.1), and (259.5 ± 8.1) nm, respectively, and the average Zeta-potential values were (–25.0 ± 1.6), (–21.4 ± 0.6), and (–22.4 ± 1.6) mV, respectively (Figs. 1A and B). SEC treatment led to EVs with smaller particle sizes and more negative charges. The increase in the magnitude of the Zeta-potential after SEC treatment may lead to improvements in the aggregation stability of the EVs.

The total protein contents of the 3 kinds of concentrated and purified M-EVs were then measured (Fig. 1C). The protein contents of the concentrated Sc-EVs, Ch-EVs, and Sp-EVs (TFF treated) were (545 ± 45), (654 ± 31), and (760 ± 15) μg/mL, respectively, whereas the protein contents of the purified samples (TFF and SEC treated) decreased to (254 ± 24), (386 ± 44), (569.6 ± 7.3) μg/mL, respectively. These results suggest that the TFF treatment effectively concentrated the M-EVs, but some proteins (and potentially other impurities) with high molecular weight were also retained in these concentrates. The SEC treatment appeared to be capable of removing these impurities, such as non-EV proteins. Previous researchers have also reported that a multi-step purification is more effective at purifying EVs than a single-step purification[40].

In conclusion, Sc-EVs Ch-EVs, and Sp-EVs were successfully obtained from *Scenedesmus* sp., *Chlorella* sp., and *Spirulina* sp. by using the TFF-SEC combination method. All the EVs had relatively small dimensions and were negatively charged.

3.2 Characterization and identification of M-EVs

TEM and NTA were used to further characterize the microstructure and particle quantities of the Sc-EVs Ch-EVs, and Sp-EVs. As shown in Fig. 2A, all 3 types of M-EVs were spheroidal and had a vesicular morphology, with a clear boundary layer characteristic of the presence of a lipid bilayer. As shown in Fig. 2B, the diameters of the EVs ranged from about 100 to 400 nm, which is consistent with the dynamic light scattering results discussed earlier. The particle concentrations of the Sc-EVs, Ch-EVs, and Sp-EVs were 1.43×10^9, 1.48×10^{10}, and 1.86×10^{10} particles/mL, respectively. Previous researchers have reported that microalgae contain relatively high numbers of M-EVs, i.e., 10^{11} particles/g of biomass[19]. Thus, our study shows that high levels of M-EVs can be isolated from microalgae using the TFF method. In summary, these results show that a combination of TFF and SEC could be used to isolate intact M-EVs at relatively high levels.

3.3 Lipid and protein analysis of M-EVs

The structural integrity and biological function of EVs depend on their lipid composition[41]. Our lipidomic analysis showed that phosphatidyl choline (PC), phosphatidic acid (PA), and phosphatidyl ethanolamine (PE) were the major lipids in the Sc-EVs, Ch-EVs, and Sp-EVs with differences in the levels (Fig. 2C). The Sc-EVs were rich in PC (51.96%), PE (19.586%), and PA (14.26%), the Ch-EVs were rich in PC (44.42%) and MGDG (22.76%), and the Sp-EVs were rich in PA (33.44%) and LysoPE (44.93%). The amounts of PC in the vesicles decreased in the following order: Sc-EVs > Ch-EVs > Sp-EVs, whereas the amounts of PA decreased in the following order: Sp-EVs > Sc-EVs > Ch-EVs. Previous studies suggested that PA could promote the accumulation of PC and therefore enhance the targeting of PC to the liver[37]. Thus, the lipid components in the Sc-EVs, Ch-EVs, and Sp-EVs have the potential to target hepatocytes and exert a therapeutic effect on ALD. However, further experiments are required to verify this hypothesis.

This result showed that the protein molecular in the EVs were distributed in the range from 11 to 245 kDa (Fig. 1D). Bands with molecular weights of 35, 63, and 100 kDa were observed for the Sc-EVs and 100–135 kDa were observed for the Ch-EVs. In comparison, the proteins in the Sp-EVs had a much broad range of

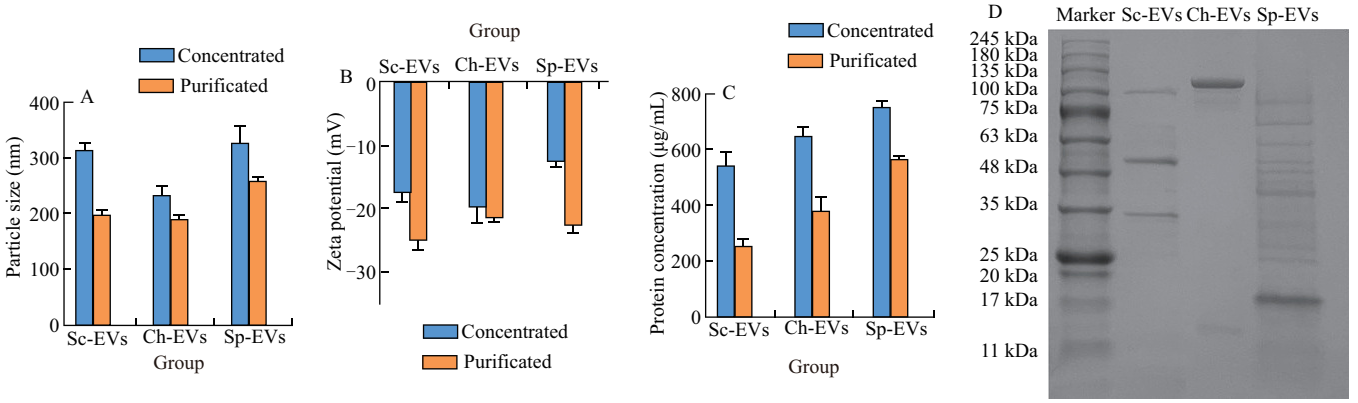

Fig. 1 Isolation and purification of 3 types of M-EVs by TFF and SEC combined method. (A) Particle size. (B) Zeta potential. (C) Concentration of concentrated and purified proteins in 3 types of M-EVs. (D) SDS-PAGE of M-EVs proteins.

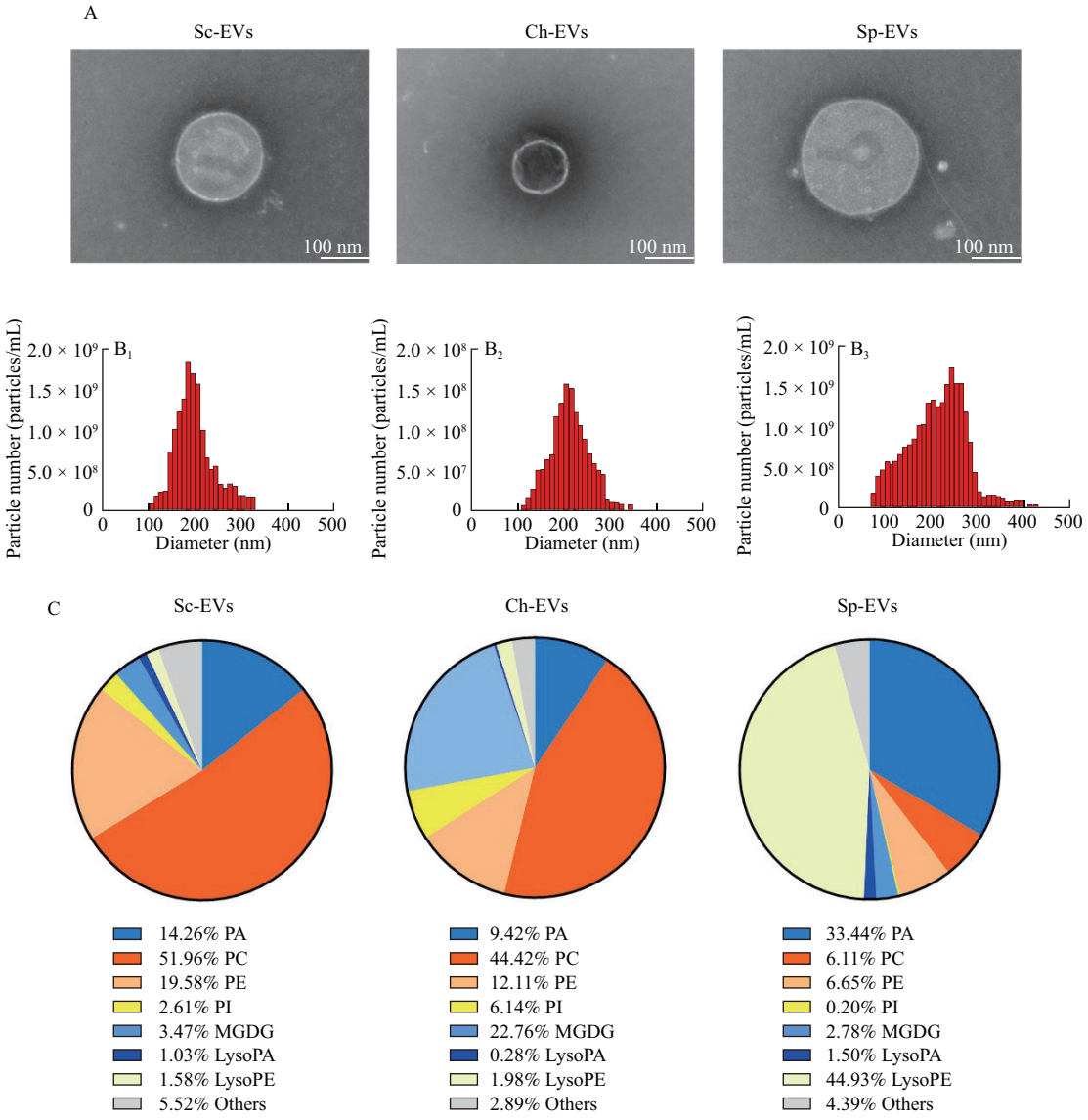

Fig. 2 Characterization and identification of three types of M-EVs. (A) Characterization of 3 types of M-EVs measured by TEM (scale bar = 100 nm). (B) Particle concentration and size distribution of 3 types of M-EVs measured by NTA. (B_1) Sc-EVs; (B_2) Ch-EVs; (B_3) Sp-EVs. (C) Lipid profile of 3 types of M-EVs indicated the percentage of total lipids. PA, phosphatidic acid; PC, phosphatidylcholine; PE, phosphatidyl ethanolamine; PI, phosphatidyl inositol; MGDG, monogalactosyl diacylglycerol; LysoPA, lysophosphatidic acid; LysoPE, lysophosphatidyl ethanolamines.

molecular weights. These results indicated that proteins of different molecular weights and compositions are present in EVs from different microalgae species, which may impact their physicochemical properties and biological activities.

3.4 *Cell viability analysis of M-EVs*

The cytotoxicity and biocompatibility of the different EVs was evaluated to assess their potential application as therapeutic agents. Caco-2 cells were treated with Sc-EVs, Ch-EVs, or Sp-EVs at concentrations of 10^7 or 10^6 particles/mL. After being incubated for 24 h with the M-EVs, the viability of the Caco-2 cells remained above 95%, which indicated no significant toxicity was observed (Fig. 3C). Moreover, there was no significant decrease in cell viability for both EV concentrations studied. Thus, it can be concluded that the 3 M-EVs exhibited favorable biocompatibility and safety.

3.5 *In vivo biodistribution of M-EVs*

To assess the *in vivo* biodistribution of the M-EVs, the fluorescence intensity of the major organs was measured, including the lungs, brain, heart, kidneys, liver, spleen, and bones. Almost no fluorescence signal was detected in the heart, while significant fluorescence signals were observed in the liver after 24 h (Fig. 3B). Interestingly, the lungs, brain, and kidneys also showed fluorescence signals for the mice treated with M-EVs. Compared to the Ch-EVs and Sp-EVs, the Sc-EVs had a wider distribution of fluorescence and clearly accumulated in the lungs, brain, kidneys, liver, and bones. Colloidal particles with different physicochemical, biochemical, and structural properties are taken up by cells through different pathways[42]. A previous study found that DiR-labelled ginger nanoparticles gave the strongest fluorescent signals in the liver, which was confirmed by immune-staining for albumin[27].

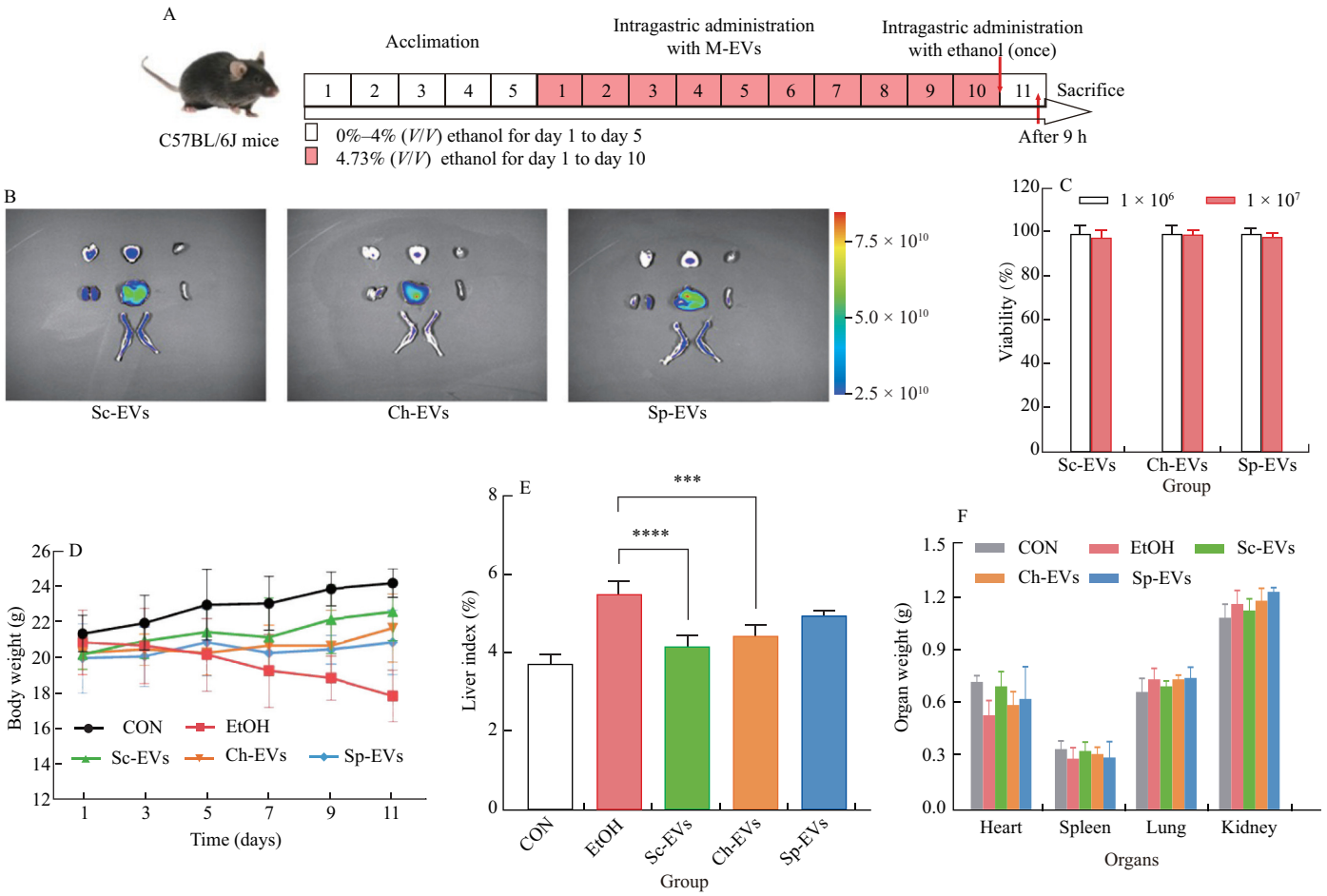

Fig. 3 *In vivo* and *in vitro* experiments of three types of M-EVs. (A) Experiment protocol for 3 types of M-EVs treatment in alcohol-induced liver injury model. (B) *In vivo* biodistribution of 3 types of M-EVs in mouse, fluorescence-based imaging experiments were performed in major organs at 24 h (lungs, brain, heart, kidneys, liver, spleen, and bones). (C) Cell viability treatment with 3 types of M-EVs *in vitro* for 24 h. (D) Body weight changes in mouse after alcohol adaptation period. (E) Liver index (liver/body weight). (F) Weight of major organs. $n = 6$ per group. ***$P < 0.001$; ****$P < 0.000\ 1$.

These results suggest that Ch-EVs, Sp-EVs, and Sc-EVs can all accumulate in the liver, which makes them suitable for treatment of ALD. Moreover, Sc-EVs may have potential for targeting and protecting other organs. It can be attributed to the fact that EVs with different biological activities are internalized by distinct types of cells, which subsequently distribute them in different organs. After that, these cells may work together to preserve organ function or tissue homeostasis[27].

3.6 *Effects of M-EVs on body weight and liver index*

An ALD mice model was established to analyze the effects of the 3 M-EVs on alcohol-induced liver injury in animals. The experimental protocol used is summarized in Fig. 3A. Over the course of the experiment, the mice in the CON group gained weight, while the mice in the EtOH group had a significant loss in body weight. This effect may be due to liver damage in mice caused by the presence of alcohol in the diet. Treatment with Sc-EVs, Ch-EVs, and Sp-EVs obviously alleviated the effects of alcohol liver damage on body weight (Fig. 3D).

The liver index is an important parameter for evaluating liver injury in animals. The EtOH group had a higher liver index than the CON group, as seen in Fig. 3E. Indeed, the liver index of the EtOH group was significantly higher than all the other groups, indicating that accumulation of fat in the liver was caused by alcohol. However, treatment with the 3 M-EVs reversed the increase in the liver index , and the Sc-EVs showed the strongest ability to reduce the liver index.

The impact of alcohol on the weights of other organs, including the heart, spleen, lung and kidney, were also measured (Fig. 3F). Increased organ weights were observed in the lungs and kidneys of the mice in the EtOH group. These changes in organ weight suggest that alcohol consumption not only damaged the liver, but also adversely affected other organs[43].

It is widely acknowledged that microalgae contain bioactive compounds that exhibit antioxidant and anti-inflammatory properties, which are beneficial to human health[44]. The bioactive molecules, including miRNA, lipids, and protein from EVs, may also affect the recipient cells in the liver and protect the liver from alcoholic damage[27,45]. M-EVs have good biosafety and biodistribution that the primary organ of action of M-EVs is the liver. In conclusion, the positive effect of M-EVs on body weight and liver index could be attributed to antioxidant and anti-inflammatory properties, which protect mice from body weight loss and liver fat during alcohol intake.

3.7 Effect of M-EVs on pathological changes in the liver

H&E staining was conducted to detect the effects of the M-EVs on alcohol-induced liver damaged. The mice in the EtOH group exhibited obvious histological changes in their liver tissue, such as loose cellular arrangement and inflammatory, the presence of macrovesicular steatosis and severe vacuolation (Fig. 4A). Slight steatosis and vacuole formation were observed in the Ch-EVs and Sp-EVs groups. However, the livers of the mice treated with the Sc-EVs displayed normal morphology with a clear boundary between hepatocytes.

Liver cell damage was also assessed using an immunofluorescence assay that utilizes uses F4/80 as a cell-surface marker unique to monocytes and macrophages (Fig. 4B). The administration of Sc-EVs, Ch-EVs, and Sp-EVs resulted in a notable reduction in macrophage infiltration within the liver. The fluorescence observed in the Sc-EVs group was comparable to that of the CON group. The average fluorescence intensity corroborated this finding (Fig. 4C). These results were therefore consistent with the H&E staining results. Thus, the 3 M-EVs, but particularly the Sc-EVs, reduced alcohol-induced liver damage.

H&E staining and immunofluorescence analysis reflected steatosis histopathological changes and hepatocellular inflammation after alcohol consumption[46]. EVs have been used to treat various disease due to its anti-inflammatory and immunomodulatory functions[26]. The different H&E results could be due to the different lipid content in EVs, which resulted in different biodistribution. It is possible for EVs to be distributed throughout the body and to be involved in a wide range of pathological processes. This is explained by the fact that the biomolecules found in EVs (such as proteins, lipids, and miRNAs) are essential for promoting intercellular communication[47]. The widely distributed of Sc-EVs may be responsible for maintaining tissue homeostasis or organ function in a coordinated manner[27]. In addition, study has reported that PC and PE exhibited antioxidant and anti-inflammatory function[45]. The combination of the aforementioned results indicates that the percentage of PC and PE in Sc-EVs is greater than that observed in Ch-EVs and Sp-EVs. In conclusion, Sc-EVs exerted greater liver protective effect than Ch-EVs and Sp-EVs because of the distribution and lipids composition.

3.8 Analysis of biochemical parameters in serum

The extent of liver damage caused by alcohol was evaluated by quantifying the levels of AST, ALT, ALP, and TG in the serum of the mice (Figs. 5A-D). A comparison between the CON and EtOH groups showed that the latter had significantly higher levels of AST, which can be attributed to the adverse effects of alcohol in their diet. A similar pattern is observed in the results for ALT, ALP, and TG levels. However, the mice in all the M-EVs groups had lower serum parameters than those in the EtOH group. In particular, the Sc-EVs group had the best effects on the ALT, AST, ALP, and TG levels. Study has showed that microalgae-derived actives with antioxidant and anti-inflammatory properties inhibited alcohol-induced elevation of ALT and AST levels[8-9,27]. In the study, the mice in all the M-EVs groups had lower serum parameters than those in the EtOH group, which were similar to previous study[48]. It was observed that PC and PE in Sc-EVs were higher than that in Ch-EVs and Sp-EVs. Study has reported that PE and PC exhibited antioxidant and anti-inflammatory properties[45]. Therefore, Sc-EVs group had the best effects on the ALT, AST, ALP, and TG, which may attribute to EVs lipids composition. These results again highlighted the potentially beneficial effects of the 3 M-EVs to prevent alcohol-induced liver damage.

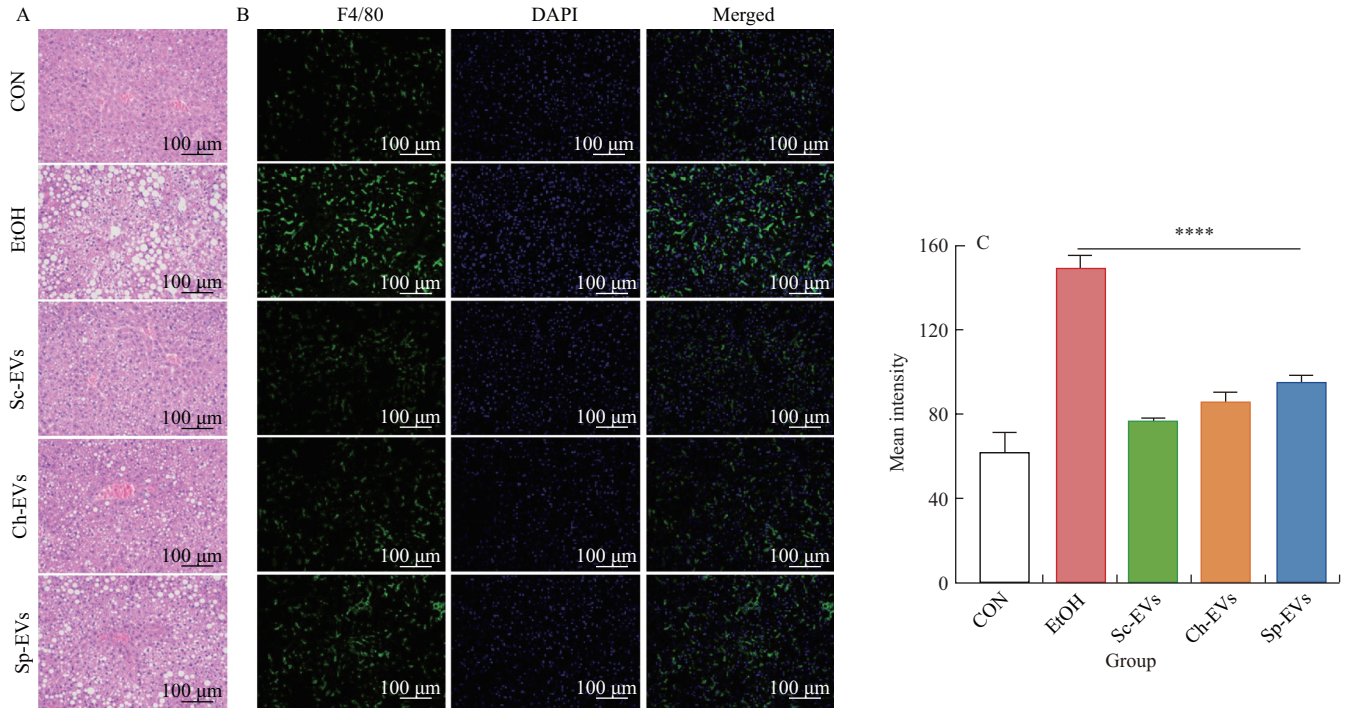

Fig. 4 Effect of three types of M-EVs on the hepatic tissue. (A) Images of the livers with H&E staining of mouse subjected to different treatments (scale bar = 100 μm). (B) Representative images of immunofluorescence staining of liver sections for F4/80 (green). The nucleus was stained with DAPI (blue). The scale bar is 100 μm. (C) Histogram of average immunofluorescence intensity. $n = 6$ per group. ****$P < 0.000\ 1$.

3.9 Effects of M-EVs on oxidative stress in the liver

The effect of oral M-EV on hepatic oxidative stress was determined by MDA, GSH and SOD assays in liver tissue. (Figs. 5E-G). The EtOH group had higher MDA levels than the CON group. Following treatment with Sc-EVs, Ch-EVs, and Sp-EVs, the MDA levels were reduced to a level approaching that of the CON group. Although GSH and SOD levels of the mice treated with all the M-EVs were elevated, the greatest increase was observed for those in the Sc-EVs group. The structure of EVs comprises a phospholipid bilayer, which contains a range of molecules, including proteins, lipids, and miRNAs. These molecules facilitate intercellular communication, thereby activating immune responses[49]. It has been previously shown that EVs could reduce the elevation of ROS and MDA levels while enhancing GSH levels against alcohol-induced oxidative stress[28]. Regarding cell viability and biodistribution studies, it was observed that M-EVs containing active compounds demonstrated favorable safety profiles and exhibited accumulation in the liver, thereby reducing oxidative stress in this organ. In conclusion, the results indicated that M-EVs protected mice from alcohol-induced oxidative stress in the liver by activating immune responses.

3.10 Effects of M-EVs on the expressions of inflammatory cytokines

The level of pro-inflammatory cytokines (TNF-α, IL-1β and IL-6) and anti-inflammatory cytokines (IL-10) were measured to assess the role of the M-EVs on inflammation expression triggered by alcoholic liver injury (Fig. 5H-K). Compared with the CON group, theEtOH group showed an increase in TNF-α, IL-1β, and IL-6 levels and a decrease in IL-10 levels. When the mice were treated with the M-EVs, levels of TNF-α, IL-1β, and IL-6 significantly decreased, which suggested that the M-EVs ameliorated the influence of pro-inflammatory cytokines triggered by alcoholic liver injury. Nevertheless, only the mice treated with Sc-EVs exhibited a notable elevation in IL-10 levels. These results showed that administration of Sc-EVs had a significant impact on inhibition of pro-inflammatory cytokines and activation of anti-inflammatory cytokines, thereby protecting the liver from alcohol-induced damage.

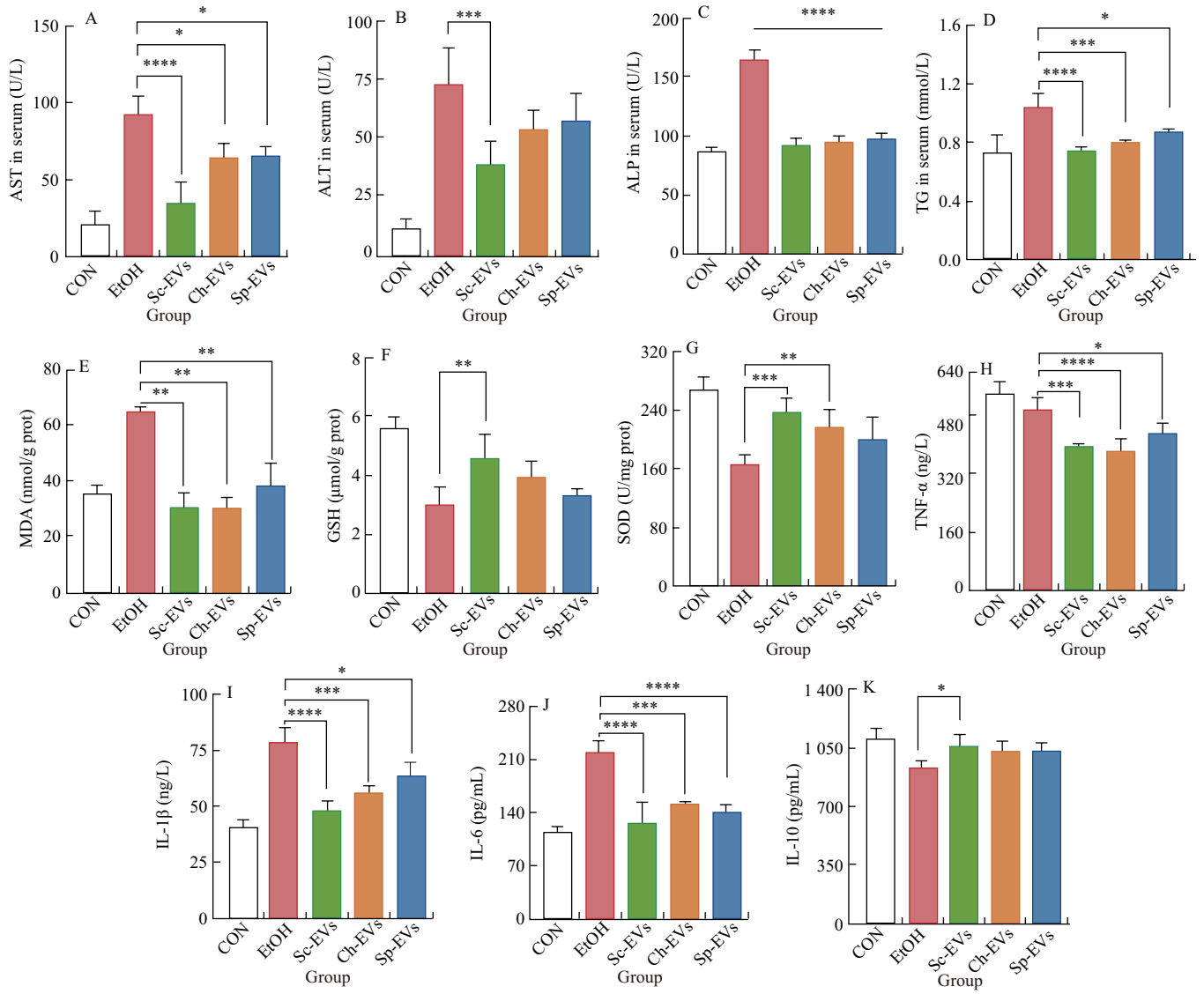

Fig. 5 Effect of 3 types of M-EVs on the biochemical parameters. (A-D) Levels of ALT, AST, ALP and TG in serum. (E-G) Levels of MDA, GSH, and SOD in liver. (H-K) Expression levels of TNF-α, IL-1β, IL-6, and IL-10 in liver determined by ELISA. n = 3–6 per group. *P < 0.05; **P < 0.01; ***P < 0.001; ****P < 0.000 1.

3.11 M-EVs reduce alcohol-induced liver injury in vivo by regulating Nrf2/HO-1/CYP2E1 signaling pathway

The potential oxidative stress mechanisms of the M-EVs on ALD were assessed by measuring the expression of Cytosolic Nrf2, Nuclear Nrf2, HO-1, and CYP2E1 in the mice liver using a Western blot analysis (Fig. 6A). Previous research has indicated that the Nrf2/HO-1 signaling pathway is a key mediator of the response of liver cells to oxidative stress[50]. When compared to the CON group, the EtOH group showed a marked decrease in Nrf2 and HO-1 expression levels. In contrast, the Sc-EVs group increased the expression levels of Nrf2 and HO-1 relative to the EtOH group. A similar tendency was observed for the Ch-EVs and Sp-EVs groups (Figs. 6B and D). CYP2E1 is regarded as a sensitive alcohol metabolizing enzyme involved in peroxide production[51]. As anticipated, the results demonstrated a significant elevation in CYP2E1 protein expression in the EtOH group relative to the CON group (Fig. 6E). However, the administration of M-EVs resulted in a significant reduction in CYP2E1 protein expression, with the Sc-EVs being the most effective.

In conclusion, the combined analysis of previous related indices of antioxidant enzymes and peroxides, including MDA, GSH, and SOD, indicated that the antioxidant protective mechanism of M-EVs on ALD was through the Nrf2/HO-1/CYP2E1 signaling pathway.

3.12 Effect of M-EVs on gut microbial diversity and composition

Alcohol intake is known to affect the number and type of gut microbes, which may have adverse health effects[2,52]. For this reason, the impact of the M-EVs on the gut microbiomes of the mice was measured. The number of common and distinct operational taxonomic units (OTUs) among the various experimental groups, as well as the overlap of ASV/OTUs, was depicted using a Venn diagram (Fig. 7A). Principal coordinate analysis (PCoA) (Fig. 7B) and nonmetric multidimensional scaling (NMDS) on the OTU level (Fig. 7C) showed that the overall microbial composition was appreciably different between the EtOH and CON groups. However, a significant shift in the gut microbial profile occurred after treatment with the M-EVs. At the phylum level, the abundance of Fusobacteriota and Proteobacteria increased and the abundance of Verrucomicrobiota, Bacteroidetes, and Firmicutes decreased in the EtOH group compared to the CON group, but these compositional changes were again considerably reversed after treatment with the M-EVs, especially the Sc-EVs (Fig. 7D). At the family level, a notable increase in Enterobacteriaceae abundance and a concomitant decrease in Erysipelotrichaceae and Akkermansiaceae abundance were observed in the EtOH group. However, following treatment with the M-EVs, it was discovered that these compositional changes were significantly reversed (Fig. 7F). Changes in the microbial community were also clearly observed in the heatmap (Figs. 7E and G). Furthermore, linear discriminant analysis (LDA) effect size (LEfSe) analysis showed an increase in the abundance of Proteobacteria, Enterococcaceae, and Enterobacteriales in the EtOH group compared to the CON group, and that treatment with M-EVs increased the Lachnospiraceae levels (Figs. 7H and I). These observed effects of the M-EVs on intestinal microbial diversity and composition suggest that the vesicles had a positive effect on regulating intestinal flora and alleviating alcohol-induced liver injury.

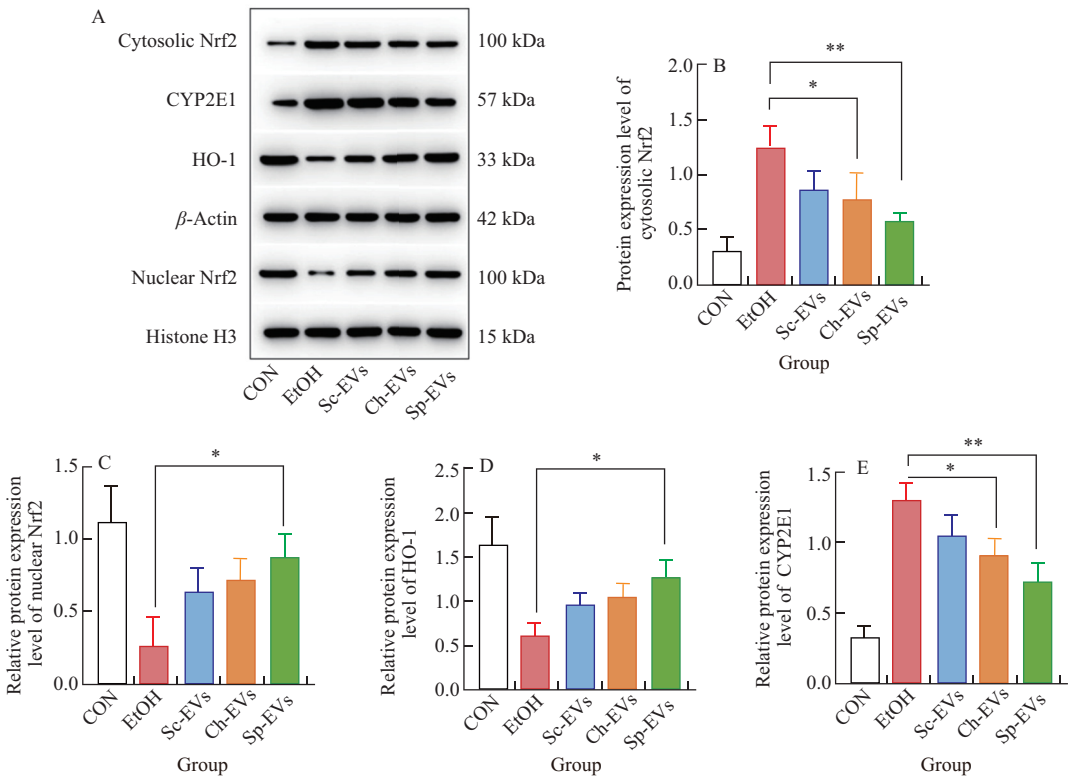

Fig. 6 Effects of three types of M-EVs on hepatic alcohol metabolism key enzymes and Nrf2/HO-1 signaling pathway. (A) Protein levels of cytosolic Nrf2, nuclear Nrf2, HO-1, and CYP2E1 in the liver tissues analyzed by Western blot. (B) Protein expression level of cytosolic Nrf2. (C) Protein expression level of nuclear Nrf2. (D) Protein expression level of HO-1. (E) Protein expression level of CYP2E1. $n = 3–5$ per group. $^{*}P < 0.05$; $^{**}P < 0.01$.

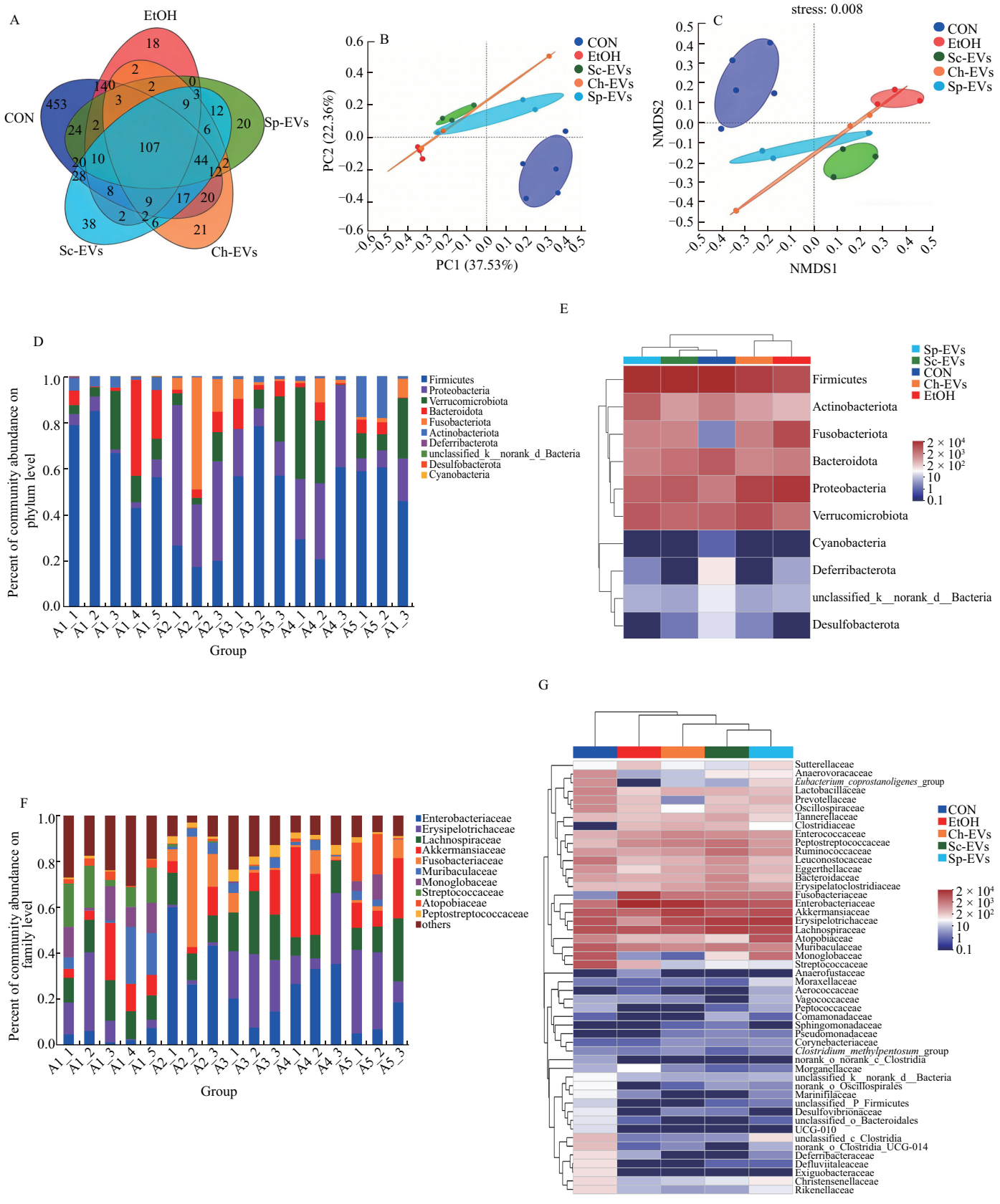

Fig. 7 Effect of 3 types of M-EVs on gut microbial diversity and composition. (A) Venn diagram of the numbers of OTUs in different experiment groups. (B) PCoA on OTU level. (C) NMDS analysis on OTU level. (D-E) Microbial community abundance and microbial community heatmap analysis at the phylum level. (F-G) Microbial community abundance and microbial community heatmap analysis at the family level. (H-I) Microbial LEfSe analysis. n = 3–5 per group.

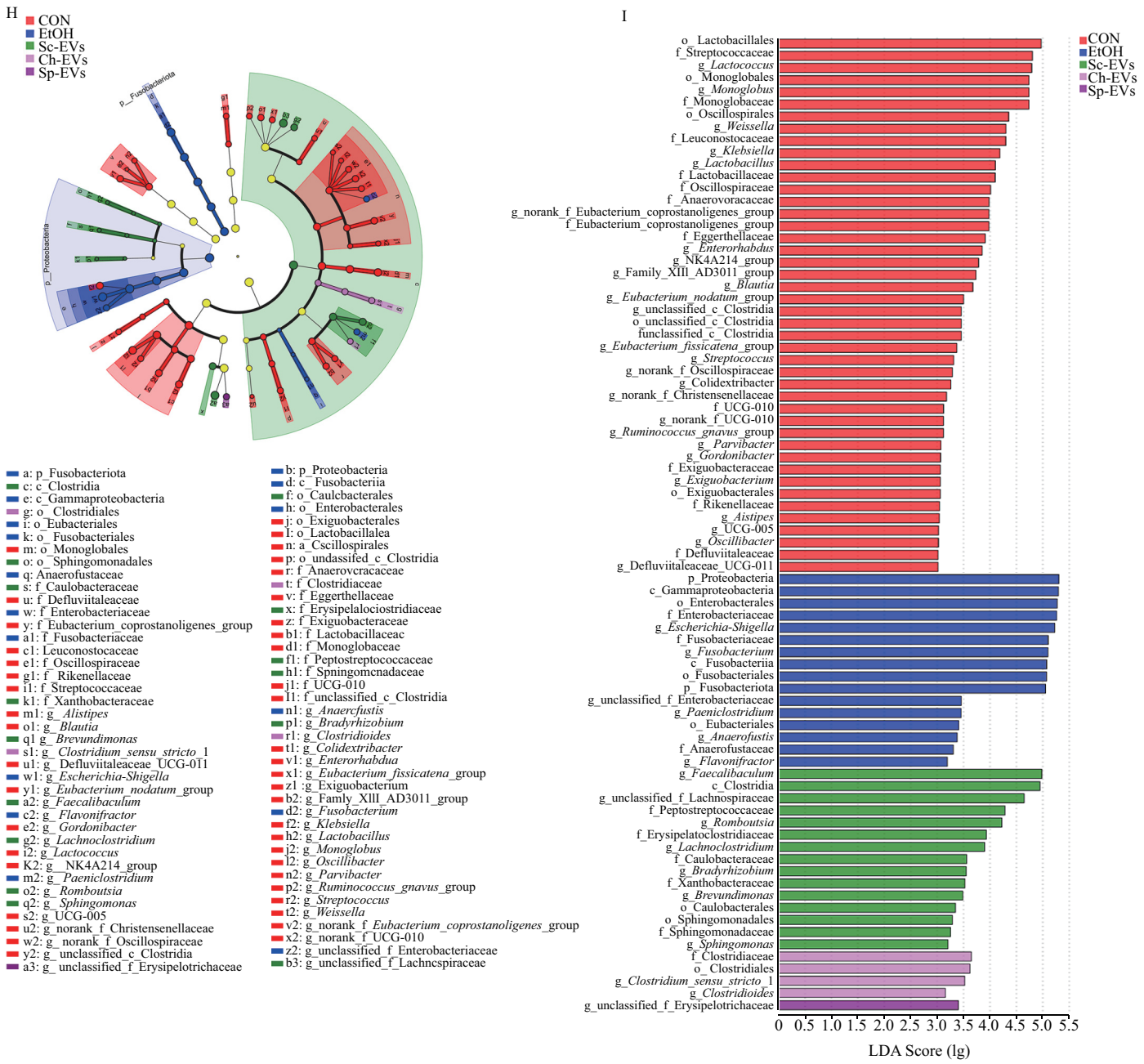

Fig. 7 (*Continued*)

4. Conclusion

In summary, microalgae as healthy ingredients for functional food, three kinds of microalgae extracellular vesicles were successfully isolated, concentrated, and purified for the first time from *Scenedesmus* sp., *Chlorella* sp., and *Spirulina* sp. using a TFF-SEC combination method. The M-EVs obtained were anionic colloidal particles with phospholipid-rich membranes, which exhibited high biocompatibility and safety. A mouse study showed that the M-EVs accumulated in the liver after oral administration. In an ALD mice model, the three types of M-EVs were shown to reduce oxidative stress and inflammation in the liver, thereby protecting it from alcohol-induced injury. Moreover, the M-EVs were shown to ameliorate hepatic oxidative stress by activating the Nrf2/HO-1 antioxidant pathway and by regulating the expression of CYP2E1. Furthermore, the protective effects of the M-EVs on ALD were related to their ability to modulate the gut microbiota by reversing the increase in harmful bacteria and decrease in beneficial bacteria that occurs after alcohol consumption.

In conclusion, this is the first demonstration that microalgal extracellular vesicles are safe, possess liver-targeting properties, and exhibit beneficial biological activities. Consequently, they have potential as therapeutic agents to alleviate the harmful effects of alcohol on the liver. Further research into the microalgae extracellular vesicles will facilitate the development of innovative application strategies in the food and human health sectors.

Declaration of competing interest

The authors declare that no competing financial interest or personal relationships that could have appeared to influence the work reported in this paper.

Acknowledgements

The authors appreciate the financial support of the National Natural Science Foundation of China (32302070), the Natural Science Foundation of Jiangxi Province (20242BAB25402), and the Key Program of National Administration of Traditional Chinese Medicine (GZY-KJS-2023034).

References

[1] H. Devarbhavi, S.K. Asrani, J.P. Arab, et al., Global burden of liver disease: 2023 update, J. Hepatol. 79 (2023) 516-537. https://doi.org/10.1016/j.jhep.2023.03.017.

[2] W. Wang, C. Xu, Q. Wang, et al., Protective effect of polyphenols, protein, peptides, and polysaccharides on alcoholic liver disease: a review of research status and molecular mechanisms, J. Agric. Food Chem. 71 (2023) 5861-5883. https://doi.org/10.1021/acs.jafc.2c07081.

[3] X. Wu, X. Fan, T. Miyata, et al., Recent advances in understanding of pathogenesis of alcohol-associated liver disease, Annu. Rev. Pathol. Mech. Dis. 18 (2023) 411-438. https://doi.org/10.1146/annurev-pathmechdis-031521-030435.

[4] Y.M. Yang, Y.E. Cho, S. Hwang, Crosstalk between oxidative stress and inflammatory liver injury in the pathogenesis of alcoholic liver disease, Int. J. Mol. Sci. 23 (2022) 774. https://doi.org/10.3390/ijms23020774.

[5] L. Abenavoli, N. Milic, S. Rouabhia, et al., Pharmacotherapy of acute alcoholic hepatitis in clinical practice, World J. Gastroenterol. 20 (2014) 2159-2167. https://doi.org/10.3748/wjg.v20.i9.2159.

[6] R. Kumar, A.S. Hegde, K. Sharma, et al., Microalgae as a sustainable source of edible proteins and bioactive peptides-current trends and future prospects, Food Res. Int. 157 (2022) 111338. https://doi.org/https://doi.org/10.1016/j.foodres.2022.111338.

[7] J. Matos, C. Cardoso, N.M. Bandarra, et al., Microalgae as healthy ingredients for functional food: a review, Food Funct. 8 (2017) 2672-2685. https://doi.org/10.1039/c7fo00409e.

[8] A.K. Koyande, K.W. Chew, K. Rambabu, et al., Microalgae: a potential alternative to health supplementation for humans, Food Sci. Hum. Wellness 8 (2019) 16-24. https://doi.org/10.1016/j.fshw.2019.03.001.

[9] J.F. Wong, H.J. Hong, S.C. Foo, et al., A review on current and future advancements for commercialized microalgae species, Food Sci. Hum. Wellness 11 (2022) 1156-1170. https://doi.org/10.1016/j.fshw.2022.04.007.

[10] T. Lafarga, J. Maria Fernandez-Sevilla, C. Gonzalez-Lopez, et al., *Spirulina* for the food and functional food industries, Food Res. Int. 137 (2020). https://doi.org/10.1016/j.foodres.2020.109356.

[11] R. Sathasivam, J.S. Ki, A review of the biological activities of microalgal carotenoids and their potential use in healthcare and cosmetic industries, Mar. Drugs 16 (2018) 26. https://doi.org/10.3390/md16010026.

[12] S.R. Chia, S.B.H.M. Nomanbhay, K.W. Chew, et al., Algae as potential feedstock for various bioenergy production, Chemosphere 287 (2022) 131944. https://doi.org/10.1016/j.chemosphere.2021.131944.

[13] K.S. Khoo, S.Y. Lee, C.W. Ooi, et al., Recent advances in biorefinery of astaxanthin from *haematococcus pluvialis*, Bioresour. Technol. 288 (2019) 121606. https://doi.org/10.1016/j.biortech.2019.121606.

[14] Q. Wu, L. Liu, A. Miron, et al., The antioxidant, immunomodulatory, and anti-inflammatory activities of spirulina: an overview, Arch. Toxicol. 90 (2016) 1817-1840. https://doi.org/10.1007/s00204-016-1744-5.

[15] S. Guzmán, A. Gato, M. Lamela, et al., Anti-inflammatory and immunomodulatory activities of polysaccharide from *Chlorella stigmatophora* and *Phaeodactylum tricomutum*, Phytother. Res. 17 (2003) 665-670. https://doi.org/10.1002/ptr.1227.

[16] T. Debnath, T.K. Bandyopadhyay, K. Vanitha, et al., Astaxanthin from microalgae: a review on structure, biosynthesis, production strategies, and application, Food Res. Int. 176 (2024) 113841. https://doi.org/https://doi.org/10.1016/j.foodres.2023.113841.

[17] T.C. do Nascimento, C.B.B. Cazarin, M.R. Maróstica, et al., Microalgae carotenoids intake: influence on cholesterol levels, lipid peroxidation and antioxidant enzymes, Food Res. Int. 128 (2020). https://doi.org/10.1016/j.foodres.2019.108770.

[18] P. Wang, X. Zheng, R. Du, et al., Astaxanthin protects against alcoholic liver injury *via* regulating mitochondrial redox balance and calcium homeostasis, J. Agric. Food Chem. 71 (2023) 19531-19550. https://doi.org/10.1021/acs.jafc.3c05529.

[19] G. Adamo, D. Fierli, D.P. Romancino, et al., Nanoalgosomes: introducing extracellular vesicles produced by microalgae, J. Extracell. Vesicles 10 (2021) e12081. https://doi.org/10.1002/jev2.12081.

[20] S. Picciotto, M.E. Barone, D. Fierli, et al., Isolation of extracellular vesicles from microalgae: towards the production of sustainable and natural nanocarriers of bioactive compounds, Biomater. Sci. 9 (2021) 2917-2930. https://doi.org/10.1039/d0bm01696a.

[21] C. Thery, K.W. Witwer, E. Aikawa, et al., Minimal information for studies of extracellular vesicles 2018 (misev2018): a position statement of the international society for extracellular vesicles and update of the misev2014 guidelines, J. Extracell. Vesicles 7 (2018) 1535750. https://doi.org/10.1080/20013078.2018.1535750.

[22] M.K. Kim, Y.C. Choi, S.H. Cho, et al., The antioxidant effect of small extracellular vesicles derived from *Aloe vera* peels for wound healing, Tissue Eng. Regen. Med. 18 (2021) 561-571. https://doi.org/10.1007/s13770-021-00367-8.

[23] D.K. Kim, W.J. Rhee, Antioxidative effects of carrot-derived nanovesicles in cardiomyoblast and neuroblastoma cells, Pharmaceutics 13 (2021) 1203. https://doi.org/10.3390/pharmaceutics13081203.

[24] F. Bayat, A. Afshar, N. Baghban, Algal cells-derived extracellular vesicles: a review with special emphasis on their antimicrobial effects, Front. Microbiol. 12 (2021) 785716. https://doi.org/10.3389/fmicb.2021.785716.

[25] A.K. Mandal, R. Nayak, B. Pradhan, et al., Algal-derived nanoparticles and their antibacterial potential: current evidence and future prospectives, J. Microbiol. Methods. 211 (2023) 106790. https://doi.org/10.1016/j.mimet.2023.106790.

[26] X. Zhou, F. Xie, L. Wang, et al., The function and clinical application of extracellular vesicles in innate immune regulation, Cell. Mol. Immunol. 17 (2020) 323-334. https://doi.org/10.1038/s41423-020-0391-1.

[27] X. Zhuang, Z.B. Deng, J. Mu, et al., Ginger-derived nanoparticles protect against alcohol-induced liver damage, J. Extracell. Vesicles 4 (2015) 28713-28713. https://doi.org/10.3402/jev.v4.28713.

[28] W. Li, S. Yang, Y. Zhao, et al., Ginseng-derived nanoparticles alleviate alcohol-induced liver injury by activating the Nrf2/HO-1 signalling pathway and inhibiting the NF-κB signalling pathway *in vitro* and *in vivo*, Phytomedicine 127 (2024) 155428. https://doi.org/10.1016/j.phymed.2024.155428.

[29] Y. Teng, J. He, Q. Zhong, et al., Grape exosome-like nanoparticles: a potential therapeutic strategy for vascular calcification, Front. Pharmacol. 13 (2022) 1025768. https://doi.org/10.3389/fphar.2022.1025768.

[30] H. Liu, J. Song, L. Zhou, et al., Construction of curcumin-fortified juices using their self-derived extracellular vesicles as natural delivery systems: grape, tomato, and orange juices, Food Funct. 14 (2023) 9364-9376. https://doi.org/10.1039/d3fo02605a.

[31] C. Wu, J. Li, K. Huang, et al., Advances in preparation and engineering of plant-derived extracellular vesicles for nutrition intervention, Food Chem. 457 (2024) 140199. https://doi.org/https://doi.org/10.1016/j.foodchem.2024.140199.

[32] A. Paterna, E. Rao, G. Adamo, et al., Isolation of extracellular vesicles from microalgae: a renewable and scalable bioprocess, Front. Bioeng. Biotechnol. 10 (2022) 836747. https://doi.org/10.3389/fbioe.2022.836747.

[33] C. Gardiner, D. Di Vizio, S. Sahoo, et al., Techniques used for the isolation and characterization of extracellular vesicles: results of a worldwide survey, J. Extracell. Vesicles 5 (2016) 32945. https://doi.org/10.3402/jev.v5.32945.

[34] J.Z. Nordin, Y. Lee, P. Vader, et al., Ultrafiltration with size-exclusion liquid chromatography for high yield isolation of extracellular vesicles preserving intact biophysical and functional properties, Nanomed. Nanotechnol. Biol. Med. 11 (2015) 879-883. https://doi.org/10.1016/j.nano.2015.01.003.

[35] E.A. Mol, M.J. Goumans, P.A. Doevendans, et al., Higher functionality of extracellular vesicles isolated using size-exclusion chromatography compared to ultracentrifugation, Nanomed. Nanotechnol. Biol. Med. 13 (2017) 2061-2065. https://doi.org/10.1016/j.nano.2017.03.011.

[36] S. Peng, Z. Li, L. Zou, et al., Enhancement of curcumin bioavailability by encapsulation in sophorolipid-coated nanoparticles: an *in vitro* and *in vivo* study, J. Agric. Food Chem. 66 (2018) 1488-1497. https://doi.org/10.1021/acs.jafc.7b05478.

[37] Y. Teng, Y. Ren, M. Sayed, et al., Plant-derived exosomal micrornas shape the gut microbiota, Cell Host Microbe. 24 (2018) 637-652. https://doi.org/10.1016/j.chom.2018.10.001.

[38] S. Busatto, G. Vilanilam, T. Ticer, et al., Tangential flow filtration for highly efficient concentration of extracellular vesicles from large volumes of fluid, Cells 7 (2018). https://doi.org/10.3390/cells7120273.

[39] M.Y. Konoshenko, E.A. Lekchnov, A.V. Vlassov, et al., Isolation of extracellular vesicles: general methodologies and latest trends, BioMed Res. Int. 2018 (2018) 8545347. https://doi.org/10.1155/2018/8545347.

[40] G. Corso, I. Mager, Y. Lee, et al., Reproducible and scalable purification of extracellular vesicles using combined bind-elute and size exclusion chromatography, Sci. Rep. 7 (2017) 11561. https://doi.org/10.1038/s41598-017-10646-x.

[41] S.Y. Hao, H.Y. Yang, J.J. Hu, et al., Bioactive compounds and biological functions of medicinal plant-derived extracellular vesicles, Pharmacol. Res. 200 (2024) 107062. https://doi.org/10.1016/j.phrs.2024.107062.

[42] Y. Liu, S. Wu, Y.J. Koo, et al., Characterization of and isolation methods for plant leaf nanovesicles and small extracellular vesicles, Nanomed. Nanotechnol. Biol. Med. 29 (2020) 102271. https://doi.org/10.1016/j.nano.2020.102271.

[43] S.H. Park, Y.S. Lee, J. Sim, et al., Alcoholic liver disease: a new insight into the pathogenesis of liver disease, Arch. Pharm. Res. 45 (2022) 447-459. https://doi.org/10.1007/s12272-022-01392-4.

[44] C.N. Eze, C.K. Onyejiaka, S.A. Ihim, et al., Bioactive compounds by microalgae and potentials for the management of some human disease conditions, AIMS Microbiol. 9 (2023) 55-74. https://doi.org/10.3934/microbiol.2023004.

[45] B.M. Wang, X.Y. Zhuang, Z.B. Deng, et al., Targeted drug delivery to intestinal macrophages by bioactive nanovesicles released from grapefruit, Mol. Ther. 22 (2014) 522-534. https://doi.org/10.1038/mt.2013.190.

[46] Z. Hua, X.D. Zhang, S.H. Xing, et al., Design and preparation of multifunctional astaxanthin nanoparticles with good acid stability and hepatocyte-targeting ability for alcoholic liver injury alleviation, Mater. Today Nano 25 (2024). https://doi.org/10.1016/j.mtnano.2023.100436.

[47] Y.C. Wang, J.F. Wang, J.Q. Ma, et al., Focusing on future applications and current challenges of plant derived extracellular vesicles, Pharmaceuticals 15 (2022) 708. https://doi.org/10.3390/ph15060708.

[48] Q.L. Yi, Z.J. Xu, A. Thakur, et al., Current understanding of plant-derived exosome-like nanoparticles in regulating the inflammatory response and immune system microenvironment, Pharmacol. Res. 190 (2023). https://doi.org/10.1016/j.phrs.2023.106733.

[49] F. Rivero-Pino, E. Marquez-Paradas, S.M. de la Paz, Food-derived vesicles as immunomodulatory drivers: current knowledge, gaps, and perspectives, Food Chem. 457 (2024) 140168. https://doi.org/10.1016/j.foodchem.2024.140168.

[50] D. Wang, J. Wang, Y. Wu, et al., Amelioration of acute alcoholic liver injury via attenuating oxidative damage and modulating inflammation by means of ursodeoxycholic acid-zein nanoparticles, J. Agric. Food Chem. 71 (2023) 17080-17096. https://doi.org/10.1021/acs.jafc.3c04786.

[51] L.Y. Zhu, M.Y. Zhang, J. Cheng, et al., *Lactiplantibacillus plantarum* and quercetin synergistically ameliorate hyperuricemia through targeting multiple pathways, Food Sci. Hum. Wellness 14 (2025) 9250264. https://doi.org/10.26599/fshw.2024.9250264.

[52] N. González-Zancada, N. Redondo-Useros, L.E. Díaz, et al., Association of moderate beer consumption with the gut microbiota and SCFA of healthy adults, Molecules 25 (2020) 4772. https://doi.org/10.3390/molecules25204772.